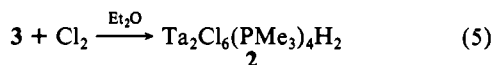
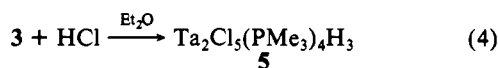
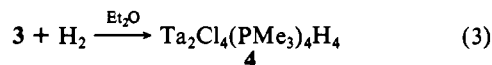


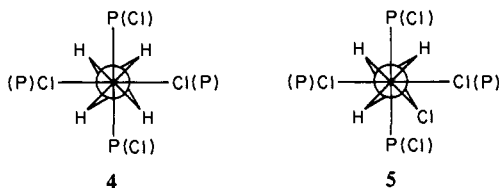
Ta(1) and 1.86 Å from Ta(2). Its density ( $\sim 0.8 \text{ e}\text{\AA}^{-3}$ ) is appropriate for a bridging hydrogen, and it lies on the diagonal plane. The Ta-H<sub>b</sub>-Ta angle is 83.1° and the shortest intramolecular contact is H<sub>b</sub>-P(5) at 2.54 Å. (2) Rotation of the hydrogen position by 45° into the all eclipsed conformation of structure A shortens the aforementioned contact to 2.02 Å. (3) The stereochemistry of the oxidative-addition products of **3** (vide infra) follows logically from structure B. (4) Molecular orbital arguments, advanced by Hoffmann and co-workers,<sup>16</sup> suggest that the staggered hydride arrangement is favored in dimers with eclipsed pyramidal end groups.

Ether solutions of **3** react readily with hydrogen, hydrogen chloride or chlorine to give the binuclear products indicated in



reactions 3-5.<sup>17</sup> These products have been characterized by elemental analyses and molecular weight measurements<sup>18,19</sup> or, in the case of Ta<sub>2</sub>Cl<sub>6</sub>(PMe<sub>3</sub>)<sub>4</sub>H<sub>2</sub> (**2**), by comparison with a sample prepared by the original route (vide supra). In the absence of definitive crystallographic proof, we suggest that Ta<sub>2</sub>Cl<sub>4</sub>(PMe<sub>3</sub>)<sub>4</sub>H<sub>4</sub> (**4**)<sup>20</sup> and Ta<sub>2</sub>Cl<sub>5</sub>(PMe<sub>3</sub>)<sub>4</sub>H<sub>3</sub> (**5**) have structures intimately related to **2**, i.e., all have similar Ta<sub>2</sub>Cl<sub>4</sub>(PMe<sub>3</sub>)<sub>4</sub> substructures, Ta-Ta single bonds, and four bridging ligands (4 H in **4**; 3 H, 1 Cl in **5**; 2 H, 2 Cl in **2**).

The NMR data on **4**<sup>18</sup> and **5**<sup>19</sup> are consistent with the end-on projections shown below. (Atoms in parenthesis are associated



with the second tantalum.) Further work on the reactivity of **3** is in progress and will be reported in the future.

In summary, we make the following observations: (1) The structure of Ta<sub>2</sub>Cl<sub>4</sub>(PMe<sub>3</sub>)<sub>4</sub>H<sub>2</sub> (**3**) represents a distinct new stereochemistry in binuclear tantalum chemistry and suggests that triply bonded eclipsed Ta<sub>2</sub>Cl<sub>4</sub>(PMe<sub>3</sub>)<sub>4</sub> is a realistic synthetic objective. (2) X-Y substrates can add across the metal-metal bond of **3**, decreasing the bond order from 2 to 1, and there are none of the gross structural rearrangements which usually accompany

(15) Bau, R.; Carroll, W. E.; Hart, D. W.; Teller, R. G.; Koetzle, T. F. *J. Am. Chem. Soc.* 1977, 99, 3872-3874.

(16) Dedieu, A.; Allbright, T. A.; Hoffmann, R. *J. Am. Chem. Soc.* 1979, 101, 3141-3151.

(17) Reaction 3 was run at 25 °C under 4 atm of hydrogen in a Fisher-Porter pressure vessel. In reactions 4 and 5, the reagent (HCl or Cl<sub>2</sub>) was dissolved in ether and added dropwise to a precooled (-20 °C) solution of **3**.

(18) Anal. Calcd for Ta<sub>2</sub>Cl<sub>4</sub>(PMe<sub>3</sub>)<sub>4</sub>H<sub>4</sub> (**4**) (Ta<sub>2</sub>Cl<sub>4</sub>P<sub>4</sub>C<sub>12</sub>H<sub>40</sub>): C, 17.75; H, 4.96; Cl, 17.46; M<sub>r</sub>, 812. Found: C, 17.61; H, 5.01; Cl, 17.39; M<sub>r</sub>, 799. NMR data: <sup>1</sup>H NMR (ppm, C<sub>6</sub>D<sub>6</sub>) 8.79 (m, 4, H<sub>b</sub>), 1.47 (m, 36, J<sub>HP</sub> ~ 4 Hz, P(CH<sub>3</sub>)<sub>3</sub>); <sup>31</sup>P NMR (ppm, C<sub>6</sub>D<sub>6</sub>, [1H]) -1.8(s); IR (cm<sup>-1</sup>, KBr disk) 1225 (m, ν<sub>Ta-H-Ta</sub>).

(19) Anal. Calcd for Ta<sub>2</sub>Cl<sub>5</sub>(PMe<sub>3</sub>)<sub>4</sub>H<sub>3</sub> (**5**) (Ta<sub>2</sub>Cl<sub>5</sub>P<sub>4</sub>C<sub>12</sub>H<sub>39</sub>): C, 17.03; H, 4.64; Cl, 20.94; M<sub>r</sub>, 846.5. Found: C, 16.89; H, 4.60; Cl, 20.95; M<sub>r</sub>, 853. NMR data: <sup>1</sup>H NMR (ppm, C<sub>6</sub>D<sub>6</sub>) 9.68 (complex m, 1, H<sub>b</sub>), 7.69 (complex m, 2, H<sub>c</sub>), 1.60 (d, 18, J<sub>PH</sub> = 9.3 Hz, P(CH<sub>3</sub>)<sub>3</sub>), 1.29 (d, 18, J<sub>PH</sub> = 8.8 Hz, P(CH<sub>3</sub>)<sub>3</sub>); <sup>31</sup>P NMR (ppm, C<sub>6</sub>D<sub>6</sub>, [1H]) +8.45 (AA'XX', m, 1, P(CH<sub>3</sub>)<sub>3</sub>), J<sub>AX} + J<sub>AX'} = 28.7 Hz), -13.34 (AA'XX', m, 1, P(CH<sub>3</sub>)<sub>3</sub>), J<sub>AX} + J<sub>AX'} = 28.7 Hz). IR (cm<sup>-1</sup>, KBr disk): 1335, 1260 (m, ν<sub>Ta-H-Ta</sub>).</sub></sub></sub></sub>

(20) (a) Ta<sub>2</sub>Cl<sub>4</sub>(PMe<sub>3</sub>)<sub>4</sub>H<sub>4</sub> (**4**) has been prepared previously by Fellmann<sup>20b</sup> and Schrock from monomeric Ta(CHCMe<sub>3</sub>)(H)Cl<sub>2</sub>(PMe<sub>3</sub>)<sub>3</sub> and molecular hydrogen. Schrock, R. R.; Fellmann, J. D., private communication. (b) Fellman, J. D. Ph.D. Thesis, Massachusetts Institute of Technology, 1980.

oxidative-addition reactions of metal-metal bonded complexes.<sup>21</sup> (3) The oxidative-addition of H<sub>2</sub>, HCl, and Cl<sub>2</sub> to a single metal-metal multiply bonded complex has no precedent in binuclear chemistry.<sup>22</sup>

**Acknowledgment.** The financial support of the U.S. Department of Energy under Grant DE-FG02-80ER10125 is gratefully acknowledged. We also thank the Marshall H. Wrubel Computing Center, Indiana University, for a generous gift of computing time. The Bruker 360 NMR spectrometer used in our research was purchased, in part, by funds provided by the National Science Foundation.

**Supplementary Material Available:** Tables of final fractional coordinates and thermal parameters (2 pages). Ordering information is given on any current masthead page.

(21) (a) Chisholm, M. H. *Transition Met. Chem.* 1978, 3, 321-333 and references therein. (b) Chisholm, M. H.; Kirkpatrick, C. C.; Huffman, J. C. *Inorg. Chem.* 1981, 20, 871-876.

(22) (a) The Mo≡Mo triple bond of [CpMo(CO)<sub>2</sub>]<sub>2</sub> will add HI and I<sub>2</sub> but not H<sub>2</sub>.<sup>22b</sup> (b) Curtis, M. D.; Messerle, L.; Fotinos, N. A.; Gerlach, R. F. In "Reactivity of Metal-Metal Bonds"; American Chemical Society: Washington, DC, 1981; ACS Symp. Ser. No. 155, Chapter 12.

## <sup>95</sup>Mo and <sup>1</sup>H ENDOR Spectroscopy of the Nitrogenase MoFe Protein

Brian M. Hoffman\* and James E. Roberts

Department of Chemistry, Northwestern University  
Evanston, Illinois 60201

W. H. Orme-Johnson\*

Department of Chemistry  
Massachusetts Institute of Technology  
Cambridge, Massachusetts 02139

Received August 24, 1981

The resting state of the nitrogenase molybdenum-iron (MoFe)<sup>1</sup> protein exhibits an EPR spectrum unique among biological systems.<sup>2</sup> It is associated with the molybdenum-iron cofactor (FeMo-co; 6-8 Fe, 4-6 S\* per molybdenum) and is characteristic of a metal center with total electron spin of  $S = 3/2$ .<sup>3</sup> Enrichment with <sup>57</sup>Fe broadens the signal, proving that the unpaired spins are associated with iron,<sup>4</sup> but lack of resolution precludes detailed analysis. Analysis of the Mössbauer effect of MoFe proteins shows that six Fe atoms are present in the  $S = 3/2$  center.<sup>4</sup> The EPR signal was not detectably broadened by enrichment with <sup>95</sup>Mo.<sup>4</sup> This shows that the signal is not associated with a simple  $S = 3/2$  Mo(II) but gives no further information about the characteristics of the molybdenum in the cofactor, although EXAFS measurements suggest that S and Fe atoms are nearby.<sup>5</sup> The modulation of electron-spin echo decay curves is affected by <sup>95</sup>Mo, but these data have been refractory to detailed analysis.<sup>6</sup> In short, present data associate the Fe with the  $S = 3/2$  center and the Mo with

(1) Abbreviations: MoFe, molybdenum-iron; FeMo-co, molybdenum-iron cofactor; EPR, electron paramagnetic resonance; ENDOR, electron nuclear double resonance.

(2) Orme-Johnson, W. H.; Hamilton, W. D.; Jones, T. L.; Tso, M.-Y. W.; Burris, R. H.; Shah, V. K.; Brill, W. J. *Proc. Natl. Acad. Sci. U.S.A.* 1972, 69, 3142-3145.

(3) Rawlings, J.; Shah, V. K.; Chisnell, J. R.; Brill, W. J.; Zimmerman, R.; Munck, E.; Orme-Johnson, W. H. *J. Biol. Chem.* 1978, 253, 1001-1004.

(4) Munck, E.; Rhodes, H.; Orme-Johnson, W. H.; Davis, L. C.; Brill, W. J.; Shah, V. K. *Biochim. Biophys. Acta* 1975, 400, 32-53.

(5) Tullius, T. D.; Conradson, S. D.; Berg, J. M.; Hodgson, K. O. In "Molybdenum Chemistry of Biological Significance"; Newton, W. E., Otsuka, S., Eds.; Plenum Press: New York, 1980.

(6) Orme-Johnson, W. H.; Peisach, J.; Mims, W. B., in progress.

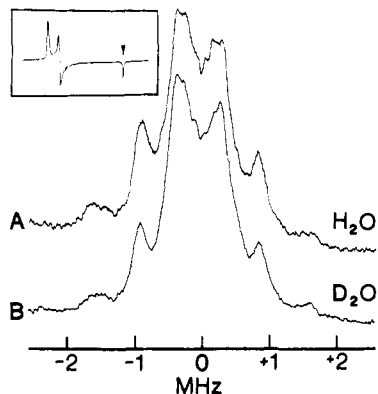


**Figure 1.** Proton ENDOR spectrum from the  $g-2$  peak of nitrogenase MoFe protein. Inset is the MoFe EPR signal, with the  $g-2$  peak to higher field indicated by an arrow and the intense, rhombically split,  $g-4$  pattern to low field. (A) ENDOR spectrum of the natural abundance protein in  $\text{H}_2\text{O}$ ; (B) ENDOR spectrum after two recrystallizations from  $\text{D}_2\text{O}$ . The frequency axis is referenced to  $\nu_{\text{H}}$ , the free-proton Larmor frequency. Conditions: 200- $\mu\text{W}$  microwave power (9.6 GHz),  $T = 2$  K, field modulation  $\approx 0.2$  G at 100 kHz, scan rate  $\sim 1$  MHz/s. Spectrum A is the summation of 650 scans and B of 1300 scans.

some (1–2) of the Fe but do not associate Mo with the  $S = 3/2$  center which is redox active during catalysis.

In several recent studies we have shown that the technique of electron nuclear double resonance (ENDOR) spectroscopy can be used to characterize the active center of a metalloenzyme.<sup>7</sup> In this communication we present the preliminary results of an ENDOR study of the resting state of the MoFe protein of nitrogenase. We have obtained well-resolved proton ENDOR signals and, of primary importance, have observed molybdenum ENDOR spectra. This provides the first spectroscopic characterization of the electronic state of the molybdenum, which is so widely expected<sup>8</sup> to occur as part of the site for  $\text{N}_2$  reduction.

Natural abundance and molybdenum-enriched nitrogenase samples were prepared as described elsewhere.<sup>4</sup> EPR and ENDOR spectra were taken in a spectrometer described previously.<sup>7</sup> The ENDOR pattern for a set of magnetically equivalent protons is a single pair of lines separated in frequency by the hyperfine coupling constant,  $A^{\text{H}}$ , and mirrored about the free-proton Larmor frequency,  $\nu_{\text{H}}$  (13.62 MHz at 3200 G).<sup>9</sup> For a set of equivalent metal (M) nuclei of spin  $I$ , the predicted ENDOR pattern consists of  $4I$  transitions with frequencies given by  $\nu(\text{obsd}) = |A^{\text{M}}/2 + P^{\text{M}}(2m-1) \pm \nu_{\text{M}}|$ , where  $-I+1 \leq m < I$  and  $P^{\text{M}}$  is the angle-dependent quadrupole splitting parameter, and all parameters can be treated as positive (absolute values). The hyperfine contribution,  $A^{\text{M}}/2$ , is invariably the largest term, and thus, for  $^{95}\text{Mo}$  ( $I = 5/2$ ,  $\nu_{\text{Mo}} = 0.88$  MHz at 3200 G), one expects 10 ENDOR lines centered at  $A^{\text{Mo}}/2$  and spanning the frequency range  $\Delta\nu = 2\nu_{\text{Mo}} + 8P^{\text{Mo}}$ .

The inset to Figure 1 shows the 4.2-K EPR spectrum of Mo Fe ( $g_x = 4.36$ ,  $g_y = 3.73$ ,  $g_z = 2.0$ ),<sup>4</sup> which is completely without any suggestion of resolved hyperfine splittings. However, setting the magnetic field to correspond to  $g = 2$  yields the weak, but well-resolved proton ENDOR spectrum (Figure 1A). Careful study of this ENDOR spectrum and others shows the existence of no fewer than five different sets of magnetically equivalent protons, with coupling constants in the range  $0.3 \lesssim A^{\text{H}} \lesssim 3.2$  MHz. The spectrum is unchanged when a sample is subjected to exhaustive  $\text{D}_2\text{O}$  exchange (Figure 1B), suggesting that these reso-

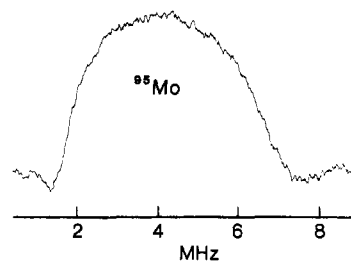


**Figure 2.**  $^{95}\text{Mo}$  ENDOR spectrum from the  $g-2$  peak of the nitrogenase MoFe protein. Spectrum was obtained by digitally subtracting the spectrum of a natural isotopic-abundance sample from that of a sample enriched to 95% with  $^{95}\text{Mo}$ . The spectrum is the summation of 1300 scans. Conditions same as Figure 1, except field modulation  $\approx 3$  G.

nances are associated with structural protons.

Figure 2 presents a low-frequency ENDOR spectrum obtained by digitally subtracting an ENDOR trace of the natural abundance sample from a trace of the  $^{95}\text{Mo}$ -enriched sample. An ENDOR peak, centered at approximately 4 MHz and spanning a frequency range of about 4.5 MHz, is clearly visible. Although the signal is broad and weaker than the resonances of Figure 1, the following observations permit us to assign it as a  $^{95}\text{Mo}$  resonance. (i) Subtractions involving several independently collected spectra of  $^{95}\text{Mo}$ -enriched and natural abundance samples yield the same feature. (ii) The resonance shifts in frequency when ENDOR is performed with the magnetic field set to correspond to  $g = 4.3$  and  $3.7$ .<sup>10</sup> (iii) When a doubly enriched sample ( $^{95}\text{Mo}$  and  $^{57}\text{Fe}$ ) is employed, subtracting the spectrum of the natural abundance protein reveals the molybdenum signal of Figure 2, along with several additional peaks ascribable to iron. (iv) These latter resonances appear when utilizing  $^{57}\text{Fe}$ -only enriched samples, but features associated with  $^{95}\text{Mo}$  do not. (v) Finally, the subtraction of two independent spectra from a natural abundance sample is featureless, demonstrating that the subtraction technique effectively eliminates consistent base-line shifts. The equation for  $\nu(\text{obsd})$  suggests the center frequency,  $\nu \sim 4.2$  MHz, is to be associated with  $A^{\text{Mo}}/2$ . However, in ENDOR simulations<sup>10</sup> of the pattern seen in Figure 2 the low-frequency half of the signal is of reduced relative intensity, as expected,<sup>9</sup> as a consequence the apparent center of the pattern is shifted to higher frequency by  $\sim 0.2$  MHz. Introducing this correction we obtain the result  $A^{\text{Mo}} \sim 8$  MHz. The individual quadrupole and nuclear Zeeman-split lines are not resolved presumably because of relatively large intrinsic metal-ENDOR linewidths. From the breadth of the pattern and the equation for  $\nu(\text{obsd})$ , we may estimate a not unreasonable<sup>11</sup> upper limit to the quadrupole coupling constant:  $P^{\text{Mo}} \sim (4.5 - 1.76)/8 \sim 3/8$  MHz.

The most important result of this study is the ENDOR observation of hyperfine couplings to molybdenum and the resulting conclusion that molybdenum is electronically integrated into the FeMo-co paramagnetic system. However, the stoichiometry of FeMo-co may also be inferred by jointly considering EPR and ENDOR data. We have performed computer simulations of the EPR spectrum assuming (i) a single molybdenum with  $A^{\text{Mo}} \lesssim 8$  MHz per  $S = 3/2$  center, (ii) two such atoms per center, (iii) two nonequivalent Mo,  $A_1^{\text{Mo}} \sim 10$  MHz and  $A_2^{\text{Mo}} \sim 6$  MHz, an assignment which could also be consistent with the ENDOR pattern of Figure 2 if the quadrupole couplings are very small. In each case the intrinsic EPR linewidth was adjusted so that the simulated  $g-2$  feature for a natural abundance sample (25%  $^{95}\text{Mo}$ ) was 28-G broad, as reported.<sup>4</sup> Then, keeping this linewidth constant, EPR spectra for a  $^{95}\text{Mo}$  enriched (95%) protein were calculated. For a single Mo per center, enrichment would broaden the EPR line by only  $<2$  G, a sufficiently small value as to be consistent with the absence of significant broadening in the experimental spectra. Assumptions ii and iii both predict a broadening of ca. 4G upon  $^{95}\text{Mo}$  enrichment: This is not consistent with experiment. We infer that the FeMo-co center contains a

(7) (a) Hoffman, B. M.; Roberts, J. E.; Brown, T. G.; Kang, C. H.; Margoliash, E. *Proc. Natl. Acad. Sci. U.S.A.* 1979, 76, 6132–6136. (b) Hoffman, B. M.; Roberts, J. E.; Swanson, M.; Spec, S. H.; Margoliash, E. *Ibid.* 1980, 77, 1452–1456. (c) Roberts, J. E.; Hoffman, B. M.; Rutter, R.; Hager, L. P. *J. Biol. Chem.* 1981, 256, 2118–2121. (d) Hoffman, B. M.; Roberts, J. E.; Kang, C. H.; Margoliash, E. *Ibid.* 1981, 256, 6556–6564.

(8) "Nitrogen Fixation"; Newton, W. E., Orme-Johnson, W. H., Eds.; University Park: Baltimore, 1980.

(9) (a) Abragam, A.; Bleaney, B. "Electron Paramagnetic Resonance of Transition Ions"; Clarendon Press: Oxford, 1970. (b) Atherton, N. M. "Electron Spin Resonance"; Wiley: New York, 1973.

(10) To be published.

(11) Vold, R. R.; Vold, R. L. *J. Chem. Phys.* 1974, 61, 4360–4361.

single molybdenum and that the resting state MoFe protein contains two such centers.

Since the observed protons are not exchangeable, they are plausibly associated with carbon-bound hydrogens of amino acid residues which coordinate to the center and link it to the protein. It is probable that one or more of these linkages is supplied by the mercaptide sulfur atoms of a metal-coordinating cysteinyl residue. The observation of a large number of protons is clearly supportive of the conclusion, obtained from analysis of the Mössbauer data,<sup>4,12</sup> that the paramagnetism of this center arises from spin coupling among the component iron atoms, now with the added requirement that molybdenum is involved, as well.

If one next considers the magnitude of the <sup>95</sup>Mo hyperfine coupling, the ENDOR results suggest that the molybdenum is to be classified as a diamagnetic, even-electron ion with even formal valency and not as Mo(V) or Mo(III). Model studies show that hyperfine couplings for an isolated, sulfur-coordinated,  $S = 1/2$  Mo(V) would be ca. 150 MHz<sup>13</sup> and that coupling constants for  $S = 3/2$  Mo(III) would be comparable.<sup>14</sup> This is roughly 20-fold larger than we observe, and thus an isolated Mo ion having either of these two formal valences is ruled out, the former case doubly so because it has the wrong spin. If the  $S = 3/2$  ground state of FeMo-co were achieved by spin coupling between an  $S = 1/2$  Mo(V) and the net spin of the six iron atoms, the intrinsic molybdenum hyperfine coupling would be strongly reduced. The reduction would be maximal (fivefold) if the resultant  $S = 3/2$  state of the center were achieved by antiferromagnetic couple of the  $S = 1/2$  molybdenum with a net iron spin of  $S = 2$ , but this model still would predict a hyperfine interaction no less than ca. four-fold larger than observed. Spin coupling between an  $S = 3/2$  Mo(III) and the net iron spin is even less favorable; a  $S = 3/2$  state obtained by antiferromagnetic coupling between  $S = 3/2$  molybdenum and a net  $S = 3$  iron spin would reduce the <sup>95</sup>Mo hyperfine interaction of an isolated molybdenum by only 40%.

Consider next the indication that the <sup>95</sup>Mo quadrupole coupling is quite small. For an atom with an unfilled d shell, the coupling is primarily determined by any unbalance in the d-orbital populations; say, for the z direction,  $P^{Mo}$  is proportional to the total of the orbital populations of  $d_{z^2}$ ,  $d_{xz}$ , and  $d_{yz}$  minus the populations of  $d_{xy}$  and  $d_{x^2-y^2}$ .<sup>15</sup> Molybdenum even-electron oxidation states in idealized geometries other than octahedral Mo(0), tetrahedral Mo(II), and Mo(VI) geometry would have a net unbalance of two d electrons. Although quadrupole data for molybdenum is scarce,<sup>11</sup> comparison with results for a variety of copper complexes,<sup>9,16</sup> taking proper notice of the difference in nuclear spins ( $I(\text{Cu}) = 3/2$ ) and the greater radial expansion of the 4d orbitals,<sup>9a</sup> suggests<sup>10</sup> that such an unbalance would produce a quadrupole coupling constant of from two to tenfold larger than the upper bound estimated above. Thus oxidation state, geometry combinations other than those three are somewhat disfavored.

In summary, the magnetic resonance data here indicate that a single molybdenum atom is integrated into the  $S = 3/2$  center of FeMo-co and that the molybdenum is best viewed as being in even-electron state, most plausibly as a nominally tetrahedral Mo(II) or a Mo(VI) ion.

**Acknowledgment.** This work has been supported by NSF Grant PCM 7681304 (B.M.H.) and NSF Grant PCM 800087330 (W.H.O.-J.) and in part by PRF Grant No. 13411-AC3 (B.M.H.). We thank Drs. Michael Henzl and Joseph Smith for helping prepare isotopically enriched nitrogenase.

(12) Huynh, B. H.; Henzl, M. T.; Christner, J. A.; Zimmerman, R.; Orme-Johnson, W. H.; Munck, E. *Biochem. Biophys. Acta* **1980**, *623*, 124-138.

(13) Hanson, G. R.; Brunette, A. A.; McDonnell, A. C.; Murray, K. S.; Wedd, A. G. *J. Am. Chem. Soc.* **1981**, *103*, 1953-1959.

(14) Averill, B. A.; Orme-Johnson, W. H. *Inorg. Chem.* **1980**, *19*, 1702-1705.

(15) (a) Townes, C. H.; Dailey, D. B. *J. Chem. Phys.* **1949**, *17*, 782. (b) Lucken, E. A. C. "Nuclear Quadrupole Coupling Constants"; Academic Press: New York, 1969.

(16) White, L. K.; Belford, R. L. *J. Am. Chem. Soc.* **1976**, *98*, 4428 and references therein.

## <sup>13</sup>C-<sup>13</sup>C Coupling Constants in Bicyclic Hydrocarbons

Ernest W. Della\* and Paul E. Pigou

School of Physical Sciences  
The Flinders University of South Australia  
Bedford Park, South Australia 5042, Australia

Received September 14, 1981

One of the more controversial aspects of carbon-carbon coupling<sup>1</sup> concerns the relative importance of the various interactions which are responsible for one-bond coupling,  $^1J(\text{CC})$ . On the one hand, a view shared by some is that spin-spin coupling between directly bonded carbon nuclei is determined predominantly by Fermi contact and, as such, is a measure of the state of hybridization of the atoms concerned.<sup>2</sup> Alternatively, attention has been drawn by others to the effect of the noncontact terms, and it has been suggested that such interactions frequently contribute significantly to the magnitude of  $^1J(\text{CC})$ , particularly in the case of multiply bonded carbons or where the atoms form part of a strained system.<sup>2</sup>

In order to provide further experimental data of coupling involving directly bonded carbons, we have synthesised for NMR analysis the bicyclic systems 1-5 ( $R = ^{13}\text{CH}_3$ )<sup>3</sup> as part of a projected series of caged compounds substituted with <sup>13</sup>C-labeled methyl at the bridgehead. At the same time we were interested in evaluating the vicinal coupling constants involving methyl and the appropriate bridgehead carbon in 2-5 ( $R = ^{13}\text{CH}_3$ ). Barfield and his colleagues<sup>4</sup> have recently demonstrated the importance of the effect of nonbonded interactions on  $^3J(\text{CC})$  in these kinds of molecules.

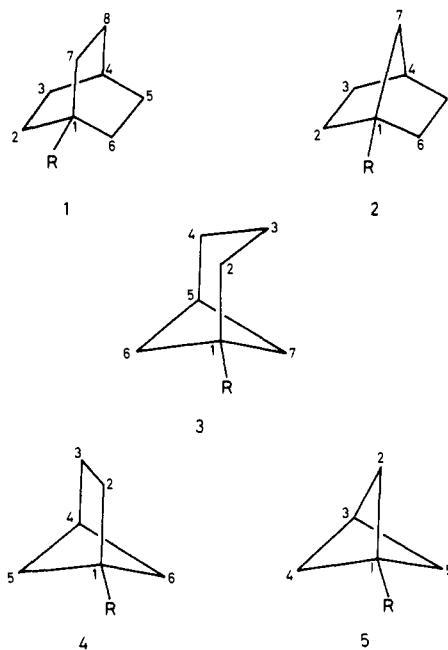


Table I contains the <sup>13</sup>C chemical shifts and Table II the various carbon-carbon coupling constants of the substrates 1-5 ( $R = ^{13}\text{CH}_3$ ). As anticipated, the features of most interest are  $^1J(\text{CC})$  and  $^3J(\text{CC})$ . For coupling between directly bonded carbons the data demonstrate that in these systems there is little correlation

(1) See (a) V. Wray in "Progress in NMR Spectroscopy", Vol. 13, J. W. Emsley, J. Feeney, and L. M. Sutcliffe, Eds., Pergamon Press, Oxford, 1979, pp 177-256; (b) P. E. Hansen and V. Wray, *Org. Magn. Reson.*, *15*, 102 (1981), and references therein for recent compilations of  $^1J(\text{CC})$  values.

(2) For leading references, see (a) H. Egli and W. von Philipsborn, *Tetrahedron Letters*, 4265 (1979); (b) T. Khin and G. A. Webb, *Org. Magn. Reson.*, *12*, 103 (1979).

(3) The syntheses and relevant properties of these hydrocarbons will be reported fully in the main paper.

(4) M. Barfield, S. E. Brown, E. D. Canada, Jr., N. D. Ledford, J. L. Marshall, S. R. Walter, and E. Yakali, *J. Am. Chem. Soc.*, *102*, 3355 (1980).